

## Density functional theory calculations of equilibrium oxygen isotope fractionation between borate minerals and aqueous fluids

Hai-Zhen WEI<sup>1,2</sup>, Martin R. PALMER<sup>3,\*</sup>, Jun-Lin WANG<sup>1</sup>, Shao-Yong JIANG<sup>4</sup>, Simon V. HOHL<sup>5</sup>,  
Yuan-Feng ZHU<sup>3</sup>, Chun HUAN<sup>1</sup>, Miao-Miao ZHANG<sup>1</sup>, Yeşim YÜCEL ÖZTÜRK<sup>6</sup>

<sup>1</sup>Department of Earth Sciences and Engineering, State Key Laboratory for Mineral Deposits Research, Nanjing University, Nanjing, PR China

<sup>2</sup>CAS Center for Excellence in Comparative Planetology, China, Anhui, P.R. China

<sup>3</sup>School of Ocean and Earth Science, University of Southampton, Southampton, UK

<sup>4</sup>Department of Earth Resources, State Key Laboratory of Geological Processes and Mineral Resources, China University of Geosciences, Wuhan, P.R. China

<sup>5</sup>State Key Laboratory of Marine Geology, Tongji University, Shanghai, P.R. China

<sup>6</sup>Department of Geological Engineering, Engineering Faculty, Dokuz Eylül University, İzmir, Türkiye

Received: 11.02.2023 • Accepted/Published Online: 01.08.2023 • Final Version: 29.09.2023

**Abstract:** Borax, ulexite, and colemanite minerals are by far the most important economic source of boron and occur almost exclusively in nonmarine evaporite deposits. While much is known about the geological setting in which they are found, surprisingly little is known about the chemical and physical properties of the brines from which they are formed. Oxygen isotope studies have the potential to reveal important new information regarding borate formation, but unlike most other common oxygen-bearing salts precipitated from brines, there are no experimental data regarding the oxygen isotope fractionation factors between borates and brines. As a first attempt to address this gap in our understanding we have determined  $\Delta^{18}\text{O}_{\text{borate-water}}$  values between 0 and 100 °C using density functional theory calculations (DFT). These results predicted  $\Delta^{18}\text{O}_{\text{borate-water}}$  values of 12.87, 22.32, and 17.5‰ at 25 °C for borax, colemanite and ulexite, respectively.

**Key words:** Oxygen isotopes, nonmarine evaporites, borax, ulexite, colemanite, borate deposits

### 1. Introduction

Borates are the most important economic source of boron (Kistler and Helvacı, 1994; Helvacı and Palmer, 2017), with Türkiye hosting approximately two-thirds of the global economic reserve. Most of the world's major borate deposits are found in nonmarine evaporate deposits formed by the evaporation of boron-rich fluids in enclosed basins in collisional tectonic settings (Helvacı, 2005). Although approximately 20 borate minerals are extracted commercially, worldwide (Garrett, 1998), the most economically important minerals are borax ( $\text{Na}_2[\text{B}_4\text{O}_5(\text{OH})_4]\cdot 8\text{H}_2\text{O}$ ), ulexite ( $\text{NaCa}[\text{B}_5\text{O}_6(\text{OH})_6]\cdot 5\text{H}_2\text{O}$ ) and colemanite ( $\text{Ca}[\text{B}_3\text{O}_4(\text{OH})_3]\cdot \text{H}_2\text{O}$ ) (Helvacı and Palmer, 2017). Because of its global prominence, much of our understanding of the formation of borate minerals has come from studies of deposits within Türkiye. These studies have revealed that the boron-rich fluids most likely derive from pooled geothermal fluids that leached boron from nearby ultrapotassic volcanic rocks and alteration of

tuff layers deposited in extensional basins (Helvacı, 2005; Palmer et al., 2019). The pooled fluids likely formed playa lakes that underwent evaporation and precipitation of the borate minerals in the sustained arid climate prevalent during the Miocene in the eastern Mediterranean region (Rouchy et al., 2006; Helvacı, 2015). Similar processes were also likely responsible for the formation of other large borate deposits in South America and China (Helvacı and Palmer, 2017).

While this general model of borate mineral formation is widely accepted, we still do not understand much about the physical and chemical conditions present in the Turkish Miocene playa lakes. For example, we do not know the temperature of the formation of the borate minerals. This is important for several reasons. For example, Palmer and Helvacı (1995; 1997) used the boron isotope compositions of colemanite, ulexite and borax to infer the pH values of the brines that precipitated these borate minerals, but in the absence of paleotemperature data they were forced to

\* Correspondence: m.r.palmer@soton.ac.uk

assume a uniform average temperature of 25 °C. While we lack quantitative paleotemperature data for the borate deposits, palynology studies suggest that the climate of the eastern Mediterranean was seasonal during the Miocene (Kayseri-Özer, 2013). As with other stable isotopes, boron isotope fractionation factors are temperature dependent; hence, this uncertainty in the paleotemperature means that the calculated pH values can only be treated as approximate at this stage.

For many minerals, the most reliable means of reconstructing their formation temperatures come from oxygen isotope studies. For example, diagenetic clay minerals (that are intercalated in many borate deposits (Helvacı, 2015)) have well-calibrated oxygen and hydrogen isotope factors (Savin and Epstein, 1970). However, no published data are available for oxygen isotope fractionation between borates and water that would allow the  $\delta^{18}\text{O}$  values of the borate minerals to be used as paleothermometers. As a first step towards addressing this knowledge gap, we have calculated oxygen isotope fractionation factors between borates and water using density functional theory calculations.

## 2. Computational methods

### 2.1 Calculation of equilibrium boron and oxygen isotope fractionation

The theories of Bigeleisen and Mayer (1947) and Urey (1947) indicate that the equilibrium isotopic fractionation due to changes in vibrational frequencies caused by the isotopic substitution in a given system can be estimated using standard thermodynamic and quantum mechanical approaches. The reduced partition function ratio (i.e. RPFRR) of isotopes of element X between phase A and monatomic ideal gas can be calculated by the harmonic approximation as follows:

$$RPFRR(X) = \frac{Z^*}{Z} = \prod_i^N \frac{u_i^* \exp\left(-\frac{u_i^*}{2}\right)}{u_i \exp(-u_i)} \frac{1 - \exp(-u_i)}{\exp\left(-\frac{u_i}{2}\right)}, \quad (\text{Eq. 1})$$

where  $Z^*$  and  $Z$  refer to the vibrational partition function for the heavy and light isotopes respectively;  $N$  is the total number of vibrational modes; the subscript  $i$  is the vibrational mode order number. For convenience, the reduced isotopic partition function ratio (RPFRR) was converted to the  $b$  factor using the relationship  $\beta = RPFRR^{1/n}$ . The exponent of  $1/n$  is a normalization factor to account for multiple substitutions in substance  $A$  containing more than one atom of  $X$ . The term of  $u_i$  ( $u_i^*$ ) was calculated from the relationship:

$$u_i = \frac{hc \times v_i}{kT}, \quad (\text{Eq. 2})$$

where  $h$  is Planck's constant,  $c$  is the speed of light,  $v_i$

is the vibrational frequency in  $\text{cm}^{-1}$ ,  $k$  is Boltzmann's constant, and  $T$  is the temperature in degrees Kelvin. The isotope fractionation at equilibrium between phases A and B can be expressed as

$$\Delta_{A-B} \sim 1000 \ln \alpha_{A-B} = 1000 \ln \beta_A - 1000 \ln \beta_B. \quad (\text{Eq. 3})$$

All calculations were carried out using the Cambridge Serial Total Energy Software Package (CASTEP) (Clark et al., 2005). The generalized-gradient approximation (GGA) method, together with the exchange-correlation functional of Perdew-Burke-Ernzerhof (PBE) (Perdew et al., 1996), and norm-conserving pseudopotentials were used for both the geometric optimizations and phonon frequency calculations for the PBC model of the minerals. The lattice parameters and calculation sets for borate minerals, including the output parameters of  $k$ -points, cut-off energy, and  $q$ -points for "fine" quality are listed in Table 1.

### 2.2. Models for minerals

#### 2.2.1. Models for borate minerals

In theoretical calculations it is important to create models to represent minerals and fluids because minerals have discrete compositions, but fluids have a continuum of compositions. For minerals, the periodic boundary conditions method is generally used to produce accurate theoretical isotope fractionations between minerals. This method has been refined within the local atomic structure of minerals and fluids to carry out electronic structure calculations of the equilibrium isotope fractionations between different minerals and aqueous solutions (Rustad et al., 2010). To calculate the stable oxygen isotope fractionation factors among colemanite, ulexite, borax and fluid, we obtained the initial crystal structure data from the American Mineralogist Crystal Structure Database (AMCSD) (<http://rruff.geo.arizona.edu/AMS/amcsd.php>). The structures of borax, colemanite and ulexite were taken from Levy and Lisensky (1978), Burns and Hawthorne (1993), and Ghose et al. (1978), respectively (Figure 1).

All initial structures were optimized using variable cell-shape molecular dynamics (Wentzcovitch, 1991) and the configurations with the lowest total energy were then selected for the vibrational frequency calculation. The results of the DFT calculation were compared with the available experimental data to examine the accuracy of the calculated phonon frequency. We also compared vibrational calculations using 23  $q$ -points in borax, which gives consistent results to those obtained using the gamma-point only in both boron and oxygen isotope fractionation.

#### 2.2.2. Computational error estimation

PBE calculations generally overestimate the experimental lattice parameters of minerals. This systematic error is typical of the PBE approximation and is usually associated

**Table 1.** The computational parameters of lattice constant, *k*-points, cut-off energy, *q*4 points and quality for frequency calculations of borate minerals.

Minerals	<i>Borax</i>	<i>Colemanite</i>	<i>Ulexite</i>
<i>a</i> (Å)	8.081	8.879	8.887
<i>b</i> (Å)	8.081	11.329	12.949
<i>c</i> (Å)	12.216	6.147	6.701
<i>a</i> (°)	102.802	90	90.193
<i>β</i> (°)	102.802	112.103	109.715
<i>γ</i> (°)	84.248	90	104.821
Volume (Å <sup>3</sup> )	757.356	572.857	698.407
<i>N</i> <sub>atoms</sub>	86	68	80
<i>K</i> -point grid			
cut-off energy (eV)	750	800	800
Quality	Fine	Fine	Fine
Formula	Na <sub>2</sub> B <sub>4</sub> O <sub>5</sub> (OH) <sub>4</sub> ·8H <sub>2</sub> O	Ca <sub>2</sub> [B <sub>3</sub> O <sub>4</sub> (OH) <sub>3</sub> ] <sub>2</sub> ·2H <sub>2</sub> O	NaCaB <sub>5</sub> O <sub>6</sub> (OH) <sub>6</sub> ·5H <sub>2</sub> O

with a systematic underestimation of the phonon frequencies (Méheut et al., 2007). Comparisons between the calculated phonon frequencies of borate minerals from this study and experimental results show that PBE calculations generally reproduce the frequencies with a systematic underestimation of up to 4%, which is in good agreement with the study by Méheut et al. (2007). According to the error analyses of Méheut et al. (2009), a relative uncertainty of the calculated frequencies of *n*% results in an uncertainty on 1000lnβ of *n*% (at low temperature) and 2*n*% (at high temperature).

According to the error estimation scheme proposed by Kowalski et al. (2013), the overall absolute errors for 1000lnβ and 1000lnα in ‰ can be estimated from  $\frac{1000\ln\beta \times 5\%}{2}$  and  $\frac{(1000\ln\beta_A + 1000\ln\beta_B) \times 5\%}{2}$ , respectively.

### 3. Results

#### 3.1. Calculation of RPFs of oxygen isotopes for borate minerals

The calculated vibrational frequencies of borate agree well with the available experimental data (Figure 2), with the slope between calculated frequencies and measured frequencies being  $0.9988 \pm 0.011$  (1σ, R<sup>2</sup> = 0.9997). The computed temperature dependences of the equilibrium oxygen isotope fractionation are shown in Figures 3a and 3b and their polynomial fitting parameters of the RPF as a function of temperature are reported in Table 2. A measure of the accuracy of vibrational calculations for borax is provided by comparing the results obtained using 23 *q*-points and the gamma-point only. The variance is

<0.36‰ at 298 K (Figure 3a), which is comparable with typical given analytical precisions for oxygen isotope values (δ<sup>18</sup>O) of ±0.5‰.

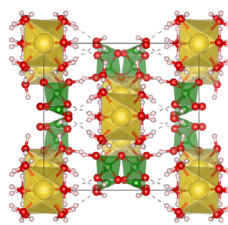
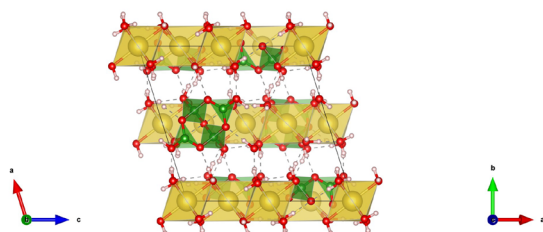
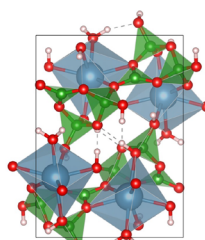
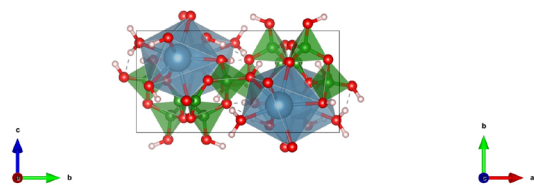
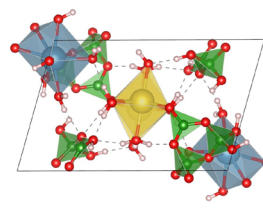
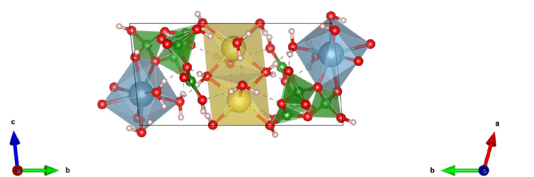
The calculated results show that colemanite is enriched in heavy oxygen isotopes (10<sup>3</sup>lnβ of 96.56‰, 298 K) and borax is enriched in <sup>11</sup>B (10<sup>3</sup>lnβ of 181.93‰, 298 K) among the three borate minerals investigated. The 10<sup>3</sup>lnβ values decrease in the sequence of colemanite > ulexite > borax (Figures 3a and 3b). The equilibrium oxygen isotope fractionation range is 4.68‰ (Δ<sup>18</sup>O<sub>colemantite-ulexite</sub>, 298 K) and 9.46‰ (Δ<sup>18</sup>O<sub>colemantite-borax</sub>, 298 K), respectively.

In addition to the boron-oxygen tetrahedron, the oxygen atoms are also distributed in crystalline water groups in the borate minerals (Figure 1). Due to the difference of the force field for oxygen atoms in the various oxygen-containing groups, the ratio of boron-oxygen groups/H<sub>2</sub>O groups in the borate minerals influences the equilibrium oxygen isotope fractionation (Figure 4).

Compared to the 10<sup>3</sup>lnβ of oxygen isotope in aqueous H<sub>2</sub>O (He et al., 2022), all the borate minerals are seen to be enriched in heavy oxygen isotopes relative to aqueous H<sub>2</sub>O. Hence the precipitating borate has a heavier δ<sup>18</sup>O value than the brine. From the calculated results, the Δ<sup>18</sup>O<sub>borate-water</sub> is 22.36‰ for colemanite, 17.68‰ for ulexite and 12.90‰ for borax at a temperature of 298 K (Figure 3b).

#### 4. Discussion and wider implications

This study has produced the first borate mineral-water oxygen isotope fractionation factors. Still, it is essential to note that they are the results of theoretical calculations and that experimental studies would be advisable to confirm

**Borax** ( $\text{Na}_2\text{B}_4\text{O}_5(\text{OH})_4 \cdot 8\text{H}_2\text{O}$ )**Colemanite** ( $\text{Ca}_2[\text{B}_3\text{O}_4(\text{OH})_3]_2 \cdot 2\text{H}_2\text{O}$ )**Ulexite** ( $\text{NaCaB}_5\text{O}_6(\text{OH})_6 \cdot 5\text{H}_2\text{O}$ )**Legend**

**Figure 1.** A series of periodic boundary cell (PBC) models for borate minerals used for the phonon frequency calculations.

the results obtained here. However, it is nontrivial to carry out such experiments under equilibrium conditions. In addition, the methods employed in this study have been successfully used to calculate a wide range of isotope fractionation factors for different elements (e.g., B, C, Mg, Ca, Fe, Ag) from Earth's surface to deep mantle conditions that show close agreement with the results of experimental studies (e.g., Rudstad et al., 2008, 2010; Rudstad and Yin, 2009; Li et al., 2020, 2021, 2022; Wang et al., 2022). Hence, the results presented here provide a sound basis for exploring the potential utility of oxygen isotope studies of borate deposits.

An additional complication to applying the theoretical oxygen isotope fractions factors (and one that would also impact experimental studies) is that the calculated  $10^3 \ln \beta$

values are the bulk values including all the oxygen atoms in the structural formulae given above. In addition to the boron-oxygen tetrahedron, the oxygen atoms are also distributed in crystalline water groups in the borate minerals (Figure 1). Due to the difference of the force field for oxygen atoms in the various oxygen-containing groups, the ratio of boron-oxygen groups/crystalline water groups in the borate minerals influences the equilibrium oxygen isotope fractionation (Figure 4). This observation will have implications for  $\delta^{18}\text{O}$  values obtained from analyses of borate minerals. If the sample was heated before analysis, causing the water groups to be driven off, the resultant  $\delta^{18}\text{O}$  values would increase above those of the pristine, hydrated mineral. This would be a particular problem for borax, which commonly loses five crystalline water

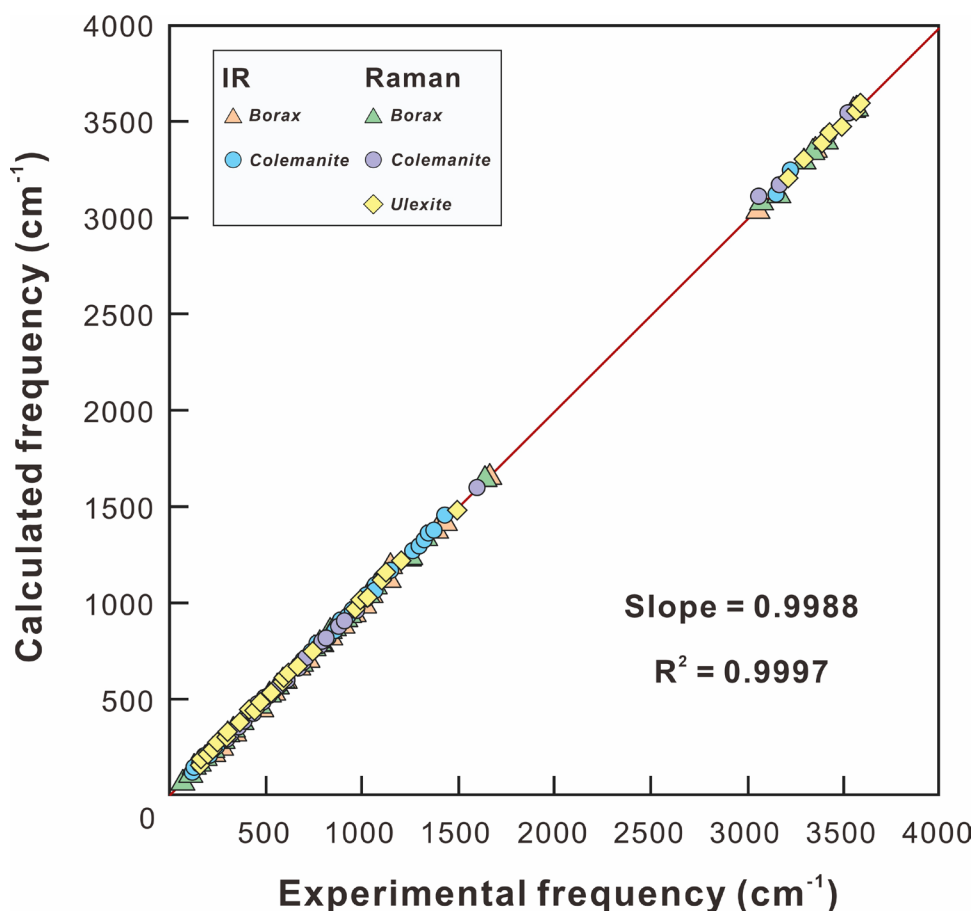


**Figure 2.** Comparison of calculated vibrational frequencies of minerals with the experimental Raman and IR data. IR data: Devi et al. (1994) for borax; Frost et al. (2013) for colemanite. Raman data: Devi et al. (1994) for borax; Frost et al. (2013) for colemanite; Kloprogge and Frost (1999) and Hurai et al. (2015) for ulexite.

groups immediately after sampling, to form tinalconite,  $\text{Na}_2\text{B}_4\text{O}_5(\text{OH})_4 \cdot 3\text{H}_2\text{O}$ . It would therefore be important that any reported  $\delta^{18}\text{O}$  data for borates contains details of whether the crystalline water groups were included in the analyses.

The primary purpose of this study is to provide an important framework for future oxygen isotope studies of borate deposits that involve analyses of borate and associated minerals. Nevertheless, it is worth noting how such studies may reveal important new information concerning borate deposit formation. The most obvious application would be determining the temperature at which the different borate minerals precipitated in a particular deposit. This would require assumptions regarding the water's oxygen isotope composition from the precipitated minerals. Still, the composition of meteoric and geothermal waters has long been well-constrained as a function of latitude and local geology (e.g., Craig, 1963).

Different borate minerals are commonly interbedded in both Turkish and South American borate deposits (Helvacı and Alonso, 2000); hence, oxygen isotope analyses of closely coexisting borate minerals may aid in determining the extent to which changes in borate mineralogy reflect changing chemical and physical conditions. Oxygen isotope analyses may also help distinguish between borate minerals in deposits that were precipitated directly from lake waters versus those that precipitated within sediments (e.g., Helvacı, 1995) as the latter would be expected to record diagenetically altered porewater oxygen isotope compositions.

## 5. Conclusion

Measurements of the oxygen isotope composition of borax, ulexite and colemanite in borate deposits can reveal important information concerning the chemical and

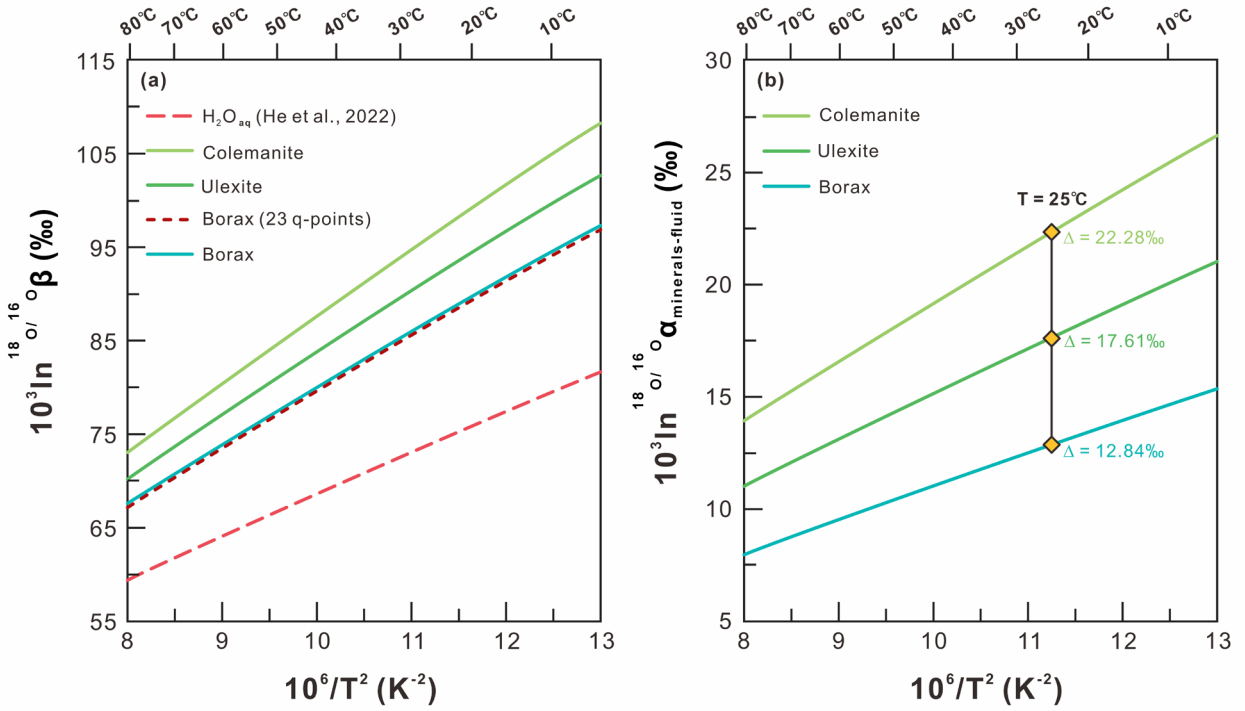


**Figure 3.** (a) The reduced partition function ratios ( $10^3 \ln \beta$ ) of  $^{18}\text{O}/^{16}\text{O}$  for borate minerals and fluid as a function of temperature ( $10^6/T^2$ ). (b) The equilibrium oxygen isotope fractionation ( $10^3 \ln \alpha_{\text{mineral-fluid}} = \Delta^{18}\text{O}_{\text{mineral-fluid}}$ ) between borate minerals and fluid as a function of temperature ( $10^6/T^2$ ).

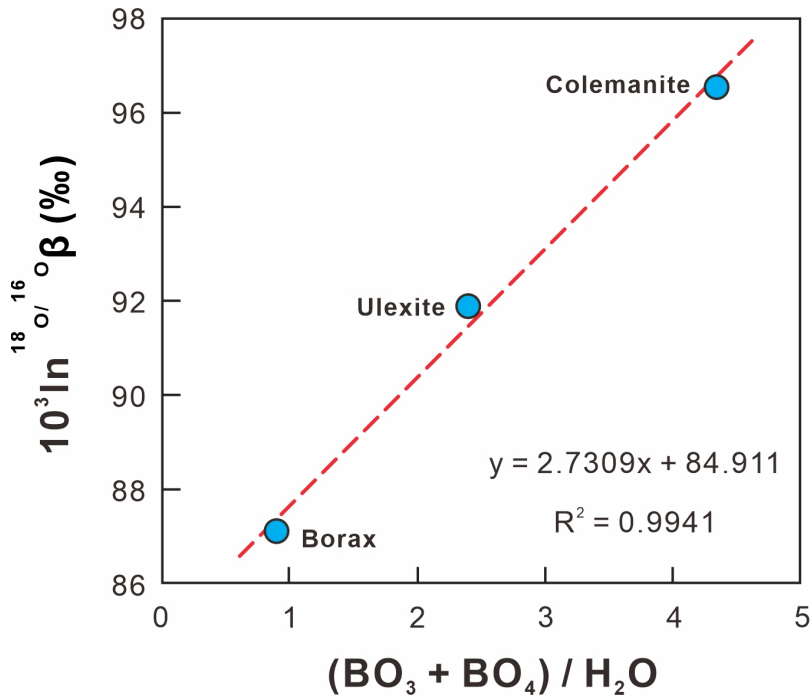


**Figure 4.** Relationship between ( $10^3 \ln \beta$ ) of  $^{18}\text{O}/^{16}\text{O}$  with ratios of B-O groups/ $\text{H}_2\text{O}$  groups in borate minerals, illustrating the influence of the force field for oxygen atoms in the various oxygen-containing groups.

**Table 2.** Polynomial fitting parameters for the relationship of ( $10^3 \ln \beta$ ) vs.  $10^6/T^2$  for borate minerals and H<sub>2</sub>O.

Mineral	<i>a</i>	<i>b</i>	<i>c</i>	<i>d</i>
Borax	0	-0.0939	7.9036	1.0280
Colemanite	0	-0.0971	9.0366	7.1285
Ulexite	0	-0.0953	8.4619	8.6972
H <sub>2</sub> O	0.0082	-0.3326	8.6720	7.0634

Note: Polynomial fitting equation:  $10^3 \ln \beta = a x^3 + b x^2 + c x + d$ , where  $x = 10^6/T^2$  and T is temperature in Kelvin. All polynomial fittings are performed between 273 K and 373 K. Values for H<sub>2</sub>O from He and Li (2022).

physical processes that led to their formation. Without experimental data for oxygen isotope fractionation factors between these borate minerals and water, we have calculated these values using density functional theory calculations. These calculations yield the following relationships for the  $\Delta^{18}\text{O}_{\text{borate-water}}$  values in per mil units between 0 and 100 °C, where T is measured in °C:

$$\Delta^{18}\text{O}_{\text{borax-water}} = 0.0004 T^2 - 0.1305 T + 15.869$$

$$\Delta^{18}\text{O}_{\text{colemanite-water}} = 0.0007 T^2 - 0.2253 T + 27.542$$

$$\Delta^{18}\text{O}_{\text{ulexite-water}} = 0.0005 T^2 - 0.1776 T + 21.750.$$

While confirmation of these theoretical oxygen isotope fractionation factors by experimental studies would be preferable, these results demonstrate that there are

significant and distinct temperature-dependent oxygen isotope fractionation factors between water and different borate minerals. Applying these results to analyses of borate minerals themselves may have important implications for furthering our understanding of the formation of borate deposits.

#### Acknowledgments

HZW acknowledges financial support by the National Science Foundation of China (Grant No. 41973005). MRP acknowledges support from NERC grant NE/V00736X/1. We are grateful to the editors and two anonymous reviewers for their helpful comments.

#### References

- Bigeleisen J, Mayer MG (1947). Calculation of equilibrium constants for isotopic exchange reactions. *Journal of Chemical Physics* 15: 261-267. <https://doi.org/10.1063/1.1746492>
- Burns PC, Hawthorne FC (1993). Hydrogen bonding in colemanite: An X-ray and structure-energy study. *Canadian Mineralogist* 31: 297-304. <https://doi.org/10.3749/1499-1276-31.2.297>
- Clark SJ, Segall MD, Pickard CJ, Hasnip PJ, Probert MI et al. (2005). First principles methods using CASTEP. *Zeitschrift für Kristallographie – Crystalline Materials* 220: 567-570. <https://doi.org/10.1524/zkri.220.5.567.65075>
- Craig H (1963). The isotopic composition of water and carbon in geothermal areas. In: Tongiorgi E (ed.) *Nuclear Geology on Geothermal Areas*, Spoleto. 17-53, Pisa, Consiglio Nazionale Della Ricerca. 284 pp.
- Devi SA, Philip D, Aruldas G (1994). Infrared, polarized Raman and SERS spectra of borax. *Journal of Solid State Chemistry* 113: 157-162. <https://doi.org/10.1006/jssc.1994.1354>
- Frost RL, Xi Y, Scholz R, Belotti FM, Filho MC (2013). Infrared and Raman spectroscopic characterization of the borate mineral colemanite – Ca<sub>3</sub>B<sub>3</sub>O<sub>4</sub>(OH)<sub>3</sub>.H<sub>2</sub>O – implications for the molecular structure. *Journal of Molecular Structure* 1037: 23-28. <https://doi.org/10.1016/j.molstruc.2012.11.047>
- Garrett DE (1998). *Borates. Handbook of Deposits, Processing, Properties and Use*. Academic Press, London, 1-483.
- Ghose S, Wan C, Clark JR (1978). Ulexite, NaCaB<sub>5</sub>O<sub>6</sub>(OH)<sub>6</sub>.5H<sub>2</sub>O: structure refinement, polyanion configuration, hydrogen bonding, and fiber optics. *American Mineralogist* 63: 160-171.
- He Y, Li L (2022). Density functional theory calculations of nitrogen and oxygen equilibrium isotope fractionations in NO<sub>3</sub> – NO<sub>2</sub> – H<sub>2</sub>O aqueous system reveal inverse kinetic isotope effects during nitrite oxidation. *Applied Geochemistry* 139: 105265. <https://doi.org/10.1016/j.apgeochem.2022.105265>
- Helvacı C (1995). Stratigraphy, mineralogy, and genesis of the Bigadiç borate deposits, western Turkey. *Economic Geology* 90: 1237-1260. <https://doi.org/10.2113/gsecongeo.90.5.1237>
- Helvacı C, Alonso RN (2000). Borate deposits of Turkey and Argentina: A summary and geological comparison. *Turkish Journal of Earth Sciences* 9: 1-27.
- Helvacı C, Palmer MR (2017). Origin and distribution of evaporite borates: The primary economic sources of boron. *Elements* 13: 249-254. <https://doi.org/10.2138/gselements.13.4.249>
- Hurav V, Huraiová M, Slobodnik M, Thomas R (2015). *Geofluids: Developments in Microthermometry, Spectroscopy, Thermodynamics, and Stable Isotopes*. Elsevier, Amsterdam 488 pp.

- Kayseri-Özer MS (2013). Spatial distribution of climatic conditions from the Middle Eocene to Late Miocene based on palynoflora in Central, Eastern and Western Anatolia. *Geodinamica Acta* 26: 122-157. <https://doi.org/10.1080/09853111.2013.877237>
- Kistler RB, Helvacı C. (1994). Boron and borates. In: Carr DD (ed.) *Industrial Minerals and Rocks*. 6th edition, Society for Mining, Metallurgy and Exploration Inc., Littleton, Colorado, 171-186. 1548 pp.
- Klopogge JT, Frost RL (1999). Raman microscopic study of some borate minerals: Ulexite, kernite, and indierite. *Applied Spectroscopy* 53: 356-364. <https://doi.org/10.1366/0003702991946587>
- Kowalski PM, Wunder B, Jahn S (2013). Ab initio prediction of equilibrium boron isotope fractionation between minerals and aqueous fluids at high P and T. *Geochimica et Cosmochimica Acta* 101: 285-301. <https://doi.org/10.1016/j.gca.2012.10.007>
- Levy HA, Lisensky GC (1978). Crystal structures of sodium sulfate decahydrate (Glauber's salt) and sodium tetraborate decahydrate (borax). Redetermination by neutron diffraction. *Acta Crystallographica Section B* B34: 3502-3510. <https://doi.org/10.1107/S0567740878011504>
- Li YC, Chen HW, Wei HZ, Jiang SY, Palmer MR et al. (2020). Exploration of driving mechanisms of equilibrium boron isotope fractionation in tourmaline group minerals and fluid: A density functional theory study. *Chemical Geology* 536: 119466. <https://doi.org/10.1016/j.chemgeo.2020.119466>
- Li YC, Wei HZ, Palmer MR, Jiang SY, Liu XJ et al. (2021). Boron coordination and B/Si ordering controls over equilibrium boron isotope fractionation among minerals, melts, and fluids. *Chemical Geology* 561: 120030. <https://doi.org/10.1016/j.chemgeo.2020.120030>
- Li YC, Wei HZ, Palmer MR, Jiang SY, Chen YX et al. (2022). Equilibrium boron isotope fractionation during serpentinization and application in understanding subduction zone processes. *Chemical Geology* 609: 121047. <https://doi.org/10.1016/j.chemgeo.2022.121047>
- Méheut M, Lazzeri M, Balan E, Mauri F (2007). Equilibrium isotopic fractionation in the kaolinite, quartz, water system: predictions from first-principles density-functional theory study. *Geochimica et Cosmochimica Acta* 71: 3170-3181. <https://doi.org/10.1016/j.gca.2007.04.012>
- Méheut M, Lazzeri M, Balan E, Mauri F (2009). Structural control over equilibrium silicon and oxygen isotopic fractionation: a first-principles density-functional theory study. *Chemical Geology* 258: 28-37. <https://doi.org/10.1016/j.chemgeo.2008.06.051>
- Palmer MR, Helvacı C (1995). The boron geochemistry of the Kirka borate deposit, western Turkey. *Geochimica et Cosmochimica Acta* 59: 3599-3605. [https://doi.org/10.1016/0016-7037\(95\)00227-Q](https://doi.org/10.1016/0016-7037(95)00227-Q)
- Palmer MR, Helvacı C (1997). The boron isotope geochemistry of the Neogene borate deposits of western Turkey. *Geochimica et Cosmochimica Acta* 61: 3161-3169. [https://doi.org/10.1016/S0016-7037\(97\)00135-X](https://doi.org/10.1016/S0016-7037(97)00135-X)
- Palmer MR, Ersoy EY, Akal C, Uysal İ, Genç ŞC et al. (2019). A short, sharp pulse of potassium-rich volcanism during continental collision and subduction. *Geology* 47: 1079-1082. <https://doi.org/10.1130/G45836.1>
- Perdew JP, Burke K, Ernzerhof M (1996). Generalized gradient approximation made simple. *Physical Review Letters* 77: 3865-3868. <https://doi.org/10.1103/PhysRevLett.77.3865>
- Rouchy JM, Caruso A (2006). The Messinian salinity crisis in the Mediterranean basin: A reassessment of the data and an integrated scenario. *Sedimentary Geology* 188-189: 35-67. <https://doi.org/10.1016/j.sedgeo.2006.02.005>
- Rudstad JR, Yin QZ (2009). Iron isotope fractionation in the Earth's lower mantle. *Nature Geoscience* 2, 514-518. <https://doi.org/10.1038/ngeo546>
- Rudstad JR, Nelmes SL, Jackson VE, Dixon DA (2008). Quantum-chemical calculations of carbon-isotope fractionation in CO<sub>2</sub>(g), aqueous carbonate species, and carbonate minerals. *Journal of Physical Chemistry A* 112, 542-555. <https://doi.org/10.1021/jp076103m>
- Rudstad JR, Casey WH, Yin QZ, Bylaska EJ, Felmy AR et al. (2010). Isotopic fractionation of Mg<sup>2+</sup>(aq), Ca<sup>2+</sup>(aq), and Fe<sup>2+</sup>(aq) with carbonate minerals. *Geochimica et Cosmochimica Acta* 74, 6301-6323. <https://doi.org/10.1016/j.gca.2010.08.018>
- Savin SM, Epstein S (1970). The oxygen and hydrogen isotope geochemistry of clay minerals. *Geochimica et Cosmochimica Acta* 34: 25-42. [https://doi.org/10.1016/0016-7037\(70\)90149-3](https://doi.org/10.1016/0016-7037(70)90149-3)
- Urey HC (1947). The thermodynamic properties of isotopic substances. *Journal of the Chemistry Society* 562-581. <https://doi.org/10.1039/jr9470000562>
- Wang JL, Wei HZ, Williams-Jones AE, Dong G, Zhu YF et al. (2022). Silver isotope fractionation in ore-forming hydrothermal systems. *Geochimica et Cosmochimica Acta* 322: 24-42. <https://doi.org/10.1016/j.gca.2022.01.024>
- Wentzcovitch RM (1991). Invariant molecular dynamics approach to structural phase transitions. *Physical Review B* 44: 2358-2361. <https://doi.org/10.1103/PhysRevB.44.2358>